Clays and Clay Minerals, Vol. 51, No. 5, 513–518, 2003.

OBSERVATION OF TWO 4-COORDINATED Al SITES IN MONTMORILLONITE USING HIGH MAGNETIC FIELD STRENGTH ^{27}Al MQMAS NMR

TAKAHIRO OHKUBO[1], KOJI KANEHASHI[2], KOJI SAITO[2] AND YASUHISA IKEDA[1,*]

[1] Research Laboratory for Nuclear Reactors, Tokyo Institute of Technology, 2-12-1 O-okayama, Meguro-ku, Tokyo 152-8550, Japan

[2] Nippon Steel Corporation, Advanced Technology Research Laboratory, 20-1 Shintomi, Futtsu City, Chiba 293-8511, Japan

Abstract—Analyses of the layer structure of Na-montmorillonite have been performed using ^{27}Al MAS and ^{27}Al MQMAS NMR techniques. Results of ^{27}Al MAS NMR measurements at higher magnetic field strength (16.4 T) suggest that the 4-coordinated Al site in Na-montmorillonite has two different structures. This was confirmed by the fact that two peaks corresponding to 4-coordinated Al are observed in the ^{27}Al MQMAS NMR at high magnetic field strength. The ratio of two 4-coordinated Al sites was found to be affected by water in the interlayer space because the area ratio of cross peaks corresponding to two 4-coordinated Al sites changes with the water content.

Key Words—^{27}Al MQMAS, High Magnetic Field Strength, Na-montmorillonite.

INTRODUCTION

Montmorillonite is a typical 2:1 type layered clay mineral and is of interest because of its properties, *e.g.* swelling with water absorption (Mooney *et al.*, 1952; Fukushima, 1984), catalyst actions (Mastalir *et al.*, 2001; Khan *et al.*, 1991; Ferris and Ertem, 1993), cation exchangeability (Staunton and Quiquampoix, 1994), and versatile applications in chemical reactions in organic media (Campanati *et al.*, 2002; Bharadwaj *et al.*, 2002). Montmorillonite contains an octahedral sheet sandwiched between two tetrahedral sheets, *i.e.* it has lamellar structure with parallel sheets of tetrahedral silicate and octahedral aluminate sheets. It is well known that isomorphic substitution of Si^{4+} by Al^{3+} occurs in the tetrahedral sheet. The properties of montmorillonite have been considered to be mainly due to the layer structures but the layer structure of montmorillonite has not been examined in sufficient detail.

High-resolution solid-state nuclear magnetic resonance (NMR) is a powerful tool for analyzing the local structure of materials. Measurements by ^{29}Si and ^{27}Al MAS (magic angle spinning) NMR have been applied to studies of the layer structures of montmorillonite (Lippmaa *et al.*, 1980; Janes and Oldfield, 1985). The ^{29}Si MAS NMR spectra have indicated that montmorillonite mainly consists of silicates with Q^3 structure, and these have been used for identification of tetrahedral structures of various clay minerals.

The ^{27}Al MAS NMR method has also been used in the structural analysis of montmorillonite, because ^{27}Al MAS NMR measurements make it possible to determine coordination numbers of Al (Müller *et al.*, 1981). However, the ^{27}Al MAS NMR spectral data are not sufficient for quantitative discussion, because the central transition (−1/2,1/2) is split by second-order quadrupolar interaction (Kundla *et al.*, 1981). Moreover, MAS NMR measurements using low spinning rate also make detailed structural analyses of montmorillonite difficult, because of overlapping of spinning side-bands (Hannus *et al.*, 1995). Of importance is the fact that the second-order quadrupolar interaction is inversely proportional to field strength (Behrens and Schnabel, 1982). Hence, MAS NMR measurements at high field strength are expected to be effective for half-integer quadrupole nuclei such as ^{27}Al.

Recently, multi-quantum (MQ) MAS NMR has been applied to structural analysis of non-crystalline materials, such as glasses (Kanehashi and Saito, 2002; Kanehashi *et al.*, 2000; Stebbins *et al.*, 2001; Fernandez and Amoureux, 1995) and aluminosilicates (Rocha, 1999; Saito *et al.*, 2001), since MQMAS NMR can average the second-order quadrupole interaction. Thus, the MQMAS technique is also expected to be useful in structural studies of tetrahedral and octahedral Al sheets in montmorillonite.

It is well known that the interlayer space of Na-montmorillonite increases noticeably with interlayer water (Hawkins and Egelstaff, 1980). In order to understand whether Al structures in tetrahedral and octahedral sheets are changed with water content, we examined hydrated and dehydrated Na-montmorillonites. In this study, we report the detailed Al structure of Na-montmorillonite using ^{27}Al MAS and MQMAS NMR techniques at high magnetic field strength.

EXPERIMENTAL

The montmorillonite used in the present study is classified as a dioctahedral smectite and was supplied by

* E-mail address of corresponding author:
yikeda@nr.titech.ac.j p
DOI: 10.1346/CCMN.2003.0510505

the Japan Clay Science Society (JCSS-3101). The chemical composition of JCSS-3101 is listed in Table 1. The internal surface area and cation exchange capacity (CEC) are 750 m^2/g and 119 meq/100 g, respectively. The exchangeable cations are Na^+ (87%), Ca^{2+} (10%) and K^+ (3%). The Na-montmorillonite was kept at room temperature under 50% humidity, and such montmorillonites are referred to as the 'original' sample in this paper. The sample of dehydrated Na-montmorillonite ('dehydrated sample') was prepared by heating an original sample at 150ºC for 48 h, and cooling to room temperature under vacuum. The dehydrated samples were packed into a NMR sample tube and analyzed.

The ^{27}Al MAS NMR measurements were performed on the Chemagnetics CMX-300 and the JEOL ECA-700 spectrometers at 7.05 T and 16.4 T. Samples were spun at 16–18 kHz in the 4 mm probes. At room temperature, the ^{27}Al MAS NMR spectra were measured using pulse-widths of 1.02 µs and 1.50 µs on the CMX-300 and the ECA-700, which correspond to 18º pulses in ^{27}Al NMR of liquid $AlCl_3$. In order to avoid drying of samples with spinning at high speed and purging with dry air to suppress any temperature increase in the sample tube accompanied by pulse radiation, the original samples were wrapped in a poly(vinylidene chloride) sheet. The dehydrated samples were analyzed without wrapping, because they were already free of water. The effectiveness of such sample treatments was confirmed by NMR spectra taken after 24 h which are consistent with those of the initial hydrated and dehydrated samples.

The ^{27}Al MQMAS NMR spectra were recorded using pulse sequences including a z-filter pulse shown in Figure 1, which is selective at low rf-powers (Amoureux *et al.*, 1996). In the MAS NMR experiment, the sample was rotated at the magic angle 54.74º, which is the angle between the static field and the rotation axis. Therefore, the chemical shift anisotropy and the dipolar interactions are averaged out, whereas the effect of second-order quadrupolar interaction is not reduced (Frydman and Harwood, 1995; Amoureux, 1993). The MQMAS NMR method can average the second-order quadrupolar interaction employing the appropriate excitation sequences. The multi-quantum coherences ±pQ (for I = 5/2, pQ can be selected as 3Q or 5Q) are excited during the evolution time t1 and the given coherence is selectively transferred to the detectable single-quantum coherence (-1)Q just before the acquisition time t2. As a result, all anisotropies can refocus in the t2-domain. The 3QMAS NMR method has been widely used in the MQMAS NMR technique, because the triple-quantum coherence is most readily excited and converted to single-quantum coherence. Typically, 5QMAS NMR experiments give higher resolution than 3QMAS NMR (Amoureux and Fernandez, 1998). Frydman and Harwood demonstrated that this multiple quantum to single quantum transfer method can yield purely isotropic spectra for half-integer quadrupole nuclei. The signal observed in MQMAS NMR depends strongly on the quadrupolar products.

Table 1. Chemical composition of clay JCSS-3101 from the Japan Clay Science Society (wt.%).

SiO_2	55.39	TiO_2	0.14
Al_2O_3	19.91	Fe_2O_3	1.57
FeO	0.37	MnO	0.01
MgO	3.40	CaO	0.52
Na_2O	3.37	K_2O	0.07
P_2O_5	0.04	H_2O	15.0
CO_2	0.45	Total	100.24

The excitation and conversion pulses were 2.8 and 1.1 µs, and were optimized independently for each sample. The MQMAS NMR experiments with the hyper complex method were carried out to obtain pure adsorption mode 2D spectra (Massiot *et al.*, 1996), in which MAS and isotropic dimensions represent cross peaks. As an alternative processing method, the sharing transformation was performed in order to obtain the isotropic and anisotropic dimensions.

Curve-fitting analyses of NMR peaks were carried out to quantify the chemical shifts and peak area by using a spectroscopic analysis program (spinsight/3, Chemagnetics and delta/4.2, JEOL USA).

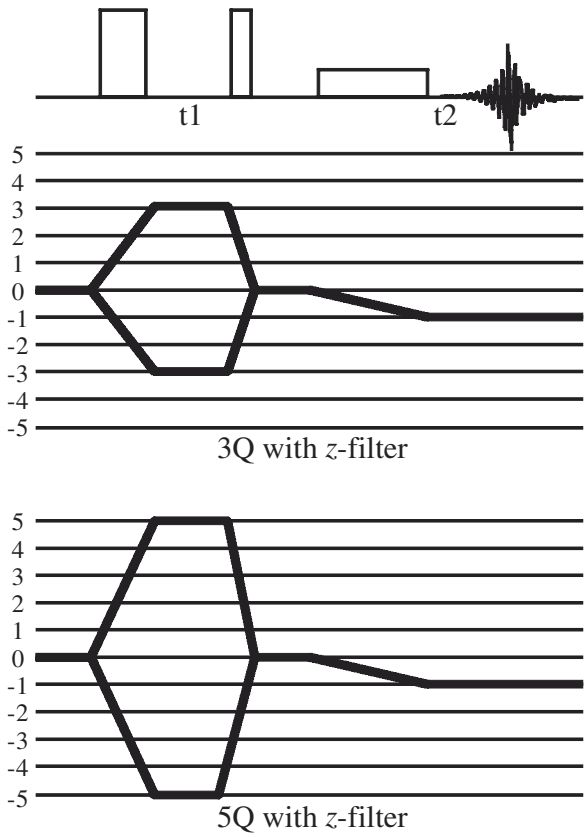

Figure 1. The pulse sequences including a z-filter pulse used for MQMAS measurements.

https://doi.org/10.1346/CCMN.2003.0510505 Published online by Cambridge University Press

Chemical shifts (ppm) were referenced to the ^{27}Al signal of a 1.0 M aqueous solution of $AlCl_3$. The error in the chemical shift is <5%.

RESULTS AND DISCUSSION

Figure 2 shows ^{27}Al MAS NMR spectra of the original sample measured at 7.05 T. As seen from Figure 2, two peaks are observed at around −0.7 ppm and ~64.3 ppm, which are assigned as ^{27}Al signals corresponding to 6- and 4-coordinated Al sites, respectively. The area ratio of 4-coordinated Al to 6-coordinated Al was determined as ~0.05 by curve-fitting to two peaks in Figure 2. Furthermore, two peaks at ~−0.7 ppm and ~64.3 ppm in Figure 2 are found to be broad and asymmetric in shape. This is supposed to be due to the effect of second-order quadrupolar interaction of ^{27}Al. Hence, we could not discuss local structures of 4- and 6-coordinated Al in detail on the basis of the ^{27}Al MAS spectrum measured at 7.05 T in Figure 2.

The MAS NMR experiments at high magnetic field strength are advantageous, because the second-order quadrupolar interaction decreases in inverse proportion to the field strength in frequency scale. In order to obtain the ^{27}Al MAS NMR spectra with higher resolution, we measured the ^{27}Al MAS NMR spectra of the same sample at 16.4 T. The result is shown in Figure 3 and found to be different from that in Figure 2, *i.e.* the line width is considerably narrower and the resonance positions are shifted to lower field. The peak area ratio of 4-coordinated Al to 6-coordinated Al was determined to be 0.09 by using the same method as described above. This result is more accurate than that in Figure 2, because the peaks of 4- and 6-coordinated Al in Figure 3 are more distinct than those in Figure 2, and in the NMR spectrum measured at high magnetic field in Figure 3 the second-quadrupolar interaction should be decreased. There have been other MAS NMR studies on montmorilllonite (Hannus *et al.*, 1995; Drachman *et al.*, 1997). The spectrum in Hannus *et al.* (1995) represents peaks corresponding to 4-coordinated Al and a superposed spinning side-band; hence there was no detailed discussion. In the Drachman *et al.* (1997) spectrum of Ca-montmorillonite, there were two peaks corresponding to 4-coordinated Al. However, they did not discuss why two peaks were observed. The interesting result in Figure 3 is that the line shape corresponding to 4-coordinated Al is asymmetric. This suggests that there are 4-coordinated Al sites with different structures in Na-montmorillonite. Unfortunately, the ^{27}Al MAS NMR spectrum is not capable of defining the difference in structure.

The MQMAS NMR technique can average absolutely the second-order quadrupolar interaction of the ^{27}Al MAS NMR spectrum. In order to examine the structures of 4-coordinated Al, we measured the ^{27}Al 3QMAS NMR spectrum of the original sample at 16.4 T. The result is shown in Figure 4. The distinct peaks of 4-coordinated Al are observed as two cross peaks. It is clear that the 4-coordinated Al in the Na-montmorillonite has two different sites. Furthermore, the 3QMAS cross peaks of 6- and 4-coordinated Al are found to spread along quadrupole-induced shift (QIS) and isotropic chemical shift (δ) axes, respectively. These results indicate that the 6-coordinated Al has an asymmetric structure and suggest that the 4-coordinated Al in

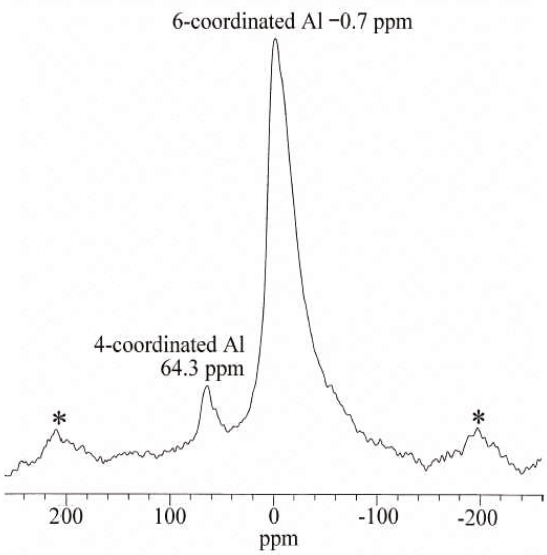

Figure 2. ^{27}Al MAS NMR spectrum of original Na-montmorillonite. Measurement conditions; spinning rate: 16 kHz, pulse delay time: 0.5 s, magnetic field: 7.05 T, 400 scans. * is spinning side-band.

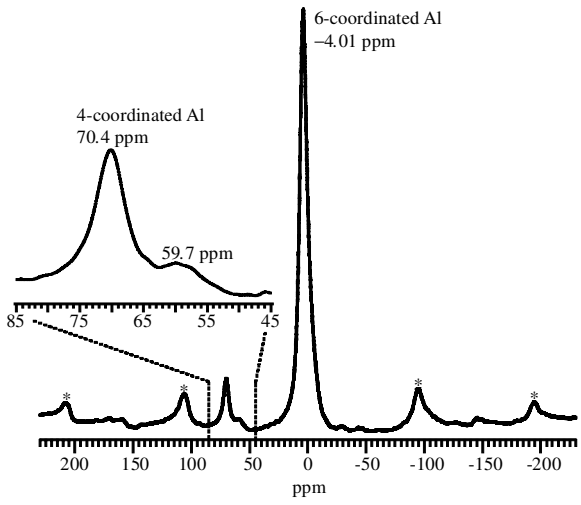

Figure 3. ^{27}Al MAS NMR spectrum of original Na-montmorillonite. Measurement conditions; spinning rate: 18 kHz, pulse delay time: 0.5 s, magnetic field: 16.4 T, 200 scans. * is spinning side-band.

https://doi.org/10.1346/CCMN.2003.0510505 Published online by Cambridge University Press

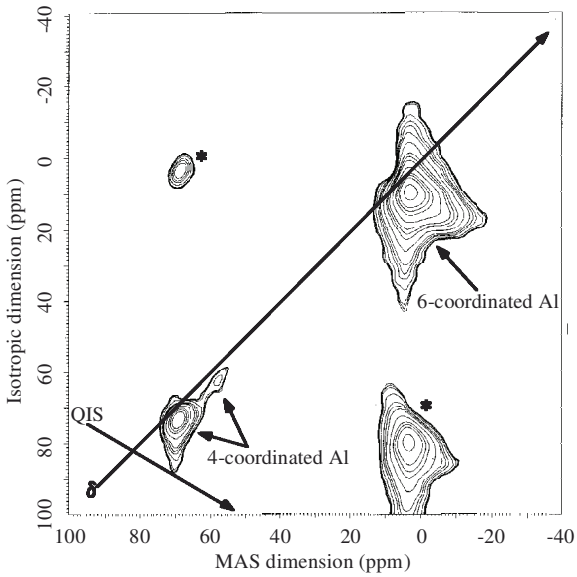

Figure 4. ^{27}Al 3QMAS NMR spectrum of original Na-montmorillonite taken under the following conditions; excitation pulse width: 2.8 μs, conversion pulse width: 1.1 μs, *z*-filter pulse width: 0.2 ms, t1 increment: 14 μs, spinning rate: 18 kHz, pulse delay: 0.3 s, magnetic field: 16.4 T, 1440 scans. * is spinning side-band.

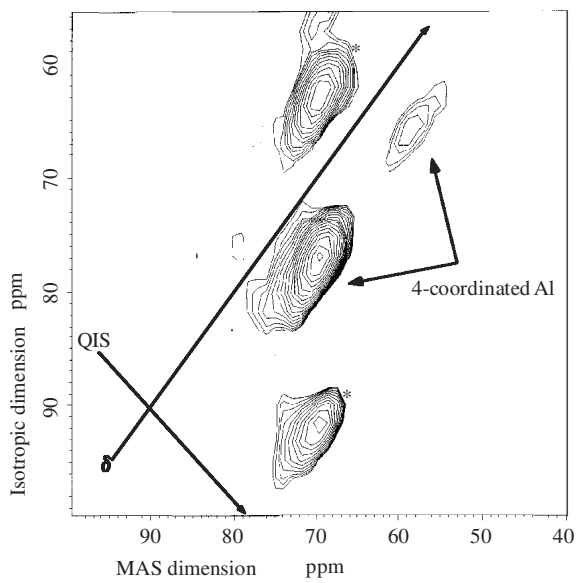

Figure 5. ^{27}Al 5QMAS NMR spectrum of original Na-montmorillonite taken under the following conditions; excitation pulse width: 2.8 μs, conversion pulse width: 1.1 μs, *z*-filter pulse width: 0.2 ms, t1 increment: 14 μs, spinning rate: 18 kHz, pulse delay: 0.3 s, magnetic field: 16.4 T, 1440 scans. * is spinning side-band.

Na-montmorillonite is distributed differently in different chemical environments. The average isotropic chemical shifts (δ_{iso}) and quadrupolar product (P_Q) were estimated from the isotropic dimension and the centers of gravity in MAS dimension of the 3QMAS line in Figure 4 using equations 1 and 2, respectively (Amoureux and Fernandez, 1998).

$$\delta_{iso} = \tfrac{10}{27}\delta_{G2}^{mas} + \tfrac{17}{27}\delta_{G1}^{iso} \quad (1)$$

$$\delta_{ISO}^{QIS} = \frac{3}{17}\frac{[4I(I+1) - 3]}{[4I(2I-1)]^2}\left(\frac{P_Q}{\omega_0}\right)\cdot 10^6 \quad (2)$$

where δ_{G2}^{mas} and δ_{G2}^{iso} are the positions (in ppm) of the centers of gravities of peaks in MAS axis and isotropic axis of the 3QMAS in Figure 4, δ_{ISO}^{QIS} is the value of quadrupole induced shift, ω_0 is the Zeeman frequency, and I is the spin quantum number. The resulting δ_{iso} and P_Q values are 9.01 ppm and 24.0 MHz for 6-coordinated Al, and 62.9 ppm, 16.7 MHz, 74.2 ppm, and 15.6 MHz for two 4-coordinated Al (I and II), respectively.

In order to confirm the validity of the above considerations, we measured the ^{27}Al 5QMAS NMR spectrum of the original sample. With the 5QMAS NMR spectra we can expect higher resolution than for 3QMAS NMR. The result is shown in Figure 5 where the 5QMAS NMR spectrum has higher resolution than that from 3QMAS in Figure 4 as expected, and two cross peaks corresponding to 4-coordinated Al are observed clearly. Therefore, it can be concluded without doubt that two sites exist for 4-coordinated Al and that the existence of two sites in Al is responsible for the observation of asymmetric shape of 4-coordinated Al in ^{27}Al MAS NMR spectrum in Figure 3.

We measured the ^{27}Al MAS NMR spectrum of the dehydrated sample to examine the effect of interlayer water on two 4-coordinated Al sites. Figure 6 shows the ^{27}Al MAS NMR spectra of the original and dehydrated samples in the range 40–90 ppm recorded at 16.4 T. The area ratio and chemical shift of two peaks (I and II) corresponding to 4-coordinated Al in the dehydrated sample seem to be different from those of the original. It was confirmed from reproducible experiments that the

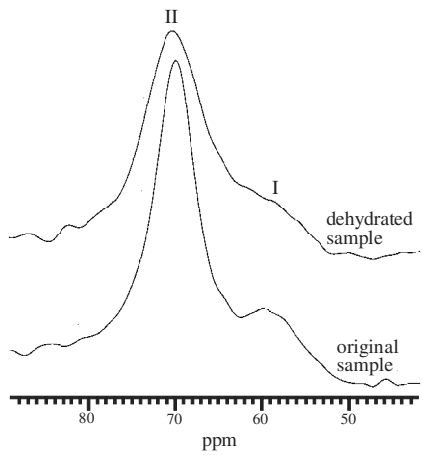

Figure 6. ^{27}Al MAS NMR spectra of original and dehydrated Na-montmorillonites recorded at 18 kHz spinning rate at 16.4 T.

https://doi.org/10.1346/CCMN.2003.0510505 Published online by Cambridge University Press

difference in chemical shift is due to the effect of the number of data sampling points. The area ratios (I/II) obtained from the curve-fitting method are 0.4 and 0.3 for dehydrated and original samples, respectively. From these results, it is considered that the 4-coordinated Al sites are specifically affected by the interlayer water, *i.e.* the peaks observed at ~60 and ~70 ppm are assigned to 4-coordinated Al which has interacted with interlayer water (~60 ppm), and that which is free from the interaction with interlayer water (~70 ppm).

Furthermore, two peaks of 4-coordinated Al in the dehydrated sample are found to be broader than those in the original sample. This is attributed to the slight structural changes in the two 4-coordinated Al sites caused by the dehydration.

CONCLUSIONS

The ^{27}Al MAS NMR spectra of Na-montmorillonite measured at 7.05 T show two peaks at ~−0.7 and 64.3 ppm, which are assigned to 6- and 4-coordinated Al, respectively. The ^{27}Al MAS NMR spectra were measured at a higher magnetic field strength of 16.4 T to decrease the effect of second-order quadrupolar interaction. As a result, the peak with asymmetric line shape assigned as 4-coordinated Al was observed at ~65 ppm. The asymmetric peak was found to be separated into two peaks (at ~60 and ~70 ppm) by using MQMAS techniques at 16.4 T. This indicates that there are two different sites for 4-coordinated Al in Na-montmorillonite. The distribution ratios of two 4-coordinated Al were found to be influenced by water content in Na-montmorillonite. From this result, it is suggested that the peaks observed at ~60 and ~70 ppm are assigned to 4-coordinated Al which interacted with interlayer water and 4-coordinated Al which did not, respectively.

REFERENCES

Amoureux, J.P. (1993) High-resolution solid-state NMR for spin 3/2 and 9/2: the multi-quantum transitions method. *Solid State Nuclear Magnetic Resonance*, **2**, 83–88.

Amoureux, J.P. and Fernandez, C. (1998) Triple, quintuple and higher order multiple quantum MAS NMR of quadrupolar nuclei. *Solid State Nuclear Magnetic Resonance*, **10**, 212–223.

Amoureux, J.P., Fernandez, C. and Steuernagel, S. (1996) Z filtering in MQMAS NMR. *Journal of Magnetic Resonance*, **A123**, 116-118.

Behrens, H.J. and Schnabel, B. (1982) The second order influence of the nuclear quadrupole interaction on the central line in the NMR of quadrupolar nuclei using rapid sample spinning. *Physica B*, **114**, 185–190.

Bharadwaj, R.K., Mehrabi, A.R., Hamilton, C., Trujillo, C., Murga, M., Fan, R., Chavira, A. and Thompson, A.K. (2002) Structure-property relationships in cross-linked polyester-clay nanocomposites. *Polymer*, **43**, 3699–3705.

Campanati, M., Casagrande, M., Fagiolino, I., Lenarda, M., Storaro, L., Battagliarin, M. and Vaccari, A. (2002) Mild hydrogenation of quinoline 2. A novel Rh-containing pillared layered clay catalyst. *Journal of Molecular Catalysis A: Chemical*, **184**, 267–272.

Drachman, S.R., Roch, G.E. and Smith, M.E. (1997) Solid state NMR characterization of the thermal transformation of Fuller's Earth. *Solid State Nuclear Magnetic Resonance*, **9**, 257–267.

Fernandez, C. and Amoureux, J.P. (1995) 2D multiquantum MAS-NMR spectroscopy of ^{27}Al in aluminophosphate molecular sieves. *Chemical Physics Letters*, **242**, 449–454.

Ferris, J.P. and Ertem, G. (1993) Montmorillonite catalysis of RNA oligomer formation in aqueous solution. A model for the prebiotic formation of RNA. *Journal of American Chemical Society*, **115**, 12270–12275.

Frydman, L. and Harwood, J.S. (1995) Isotropic spectra of half-integer quadrupolar spins from bidimensional magic-angle-spinning NMR. *Journal of American Chemical Society*, **117**, 5367–5368.

Fukushima, Y. (1984) X-ray diffraction study of aqueous montmorillonite emulsions. *Clays and Clay Minerals*, **32**, 320–326.

Hannus, I., Pálinkó, I., Lázaár, K., Nagy, J.B. and Kiricsi, I. (1995) The chemical state of Sn in Sn-montmorillonite; A multinuclear MAS NMR and ^{119}Sn Mössbauer spectroscopic study. *Journal of Molecular Structure*, **349**, 179–182.

Hawkins, R.K. and Egelstaff, P.A. (1980) Interfacial water structure in montmorillonite from neutron diffraction experiments. *Clays and Clay Minerals*, **28**, 19–28.

Janes, N. and Oldfield, E. (1985) Prediction of silicon-29 nuclear magnetic resonance chemical shifts using a group electronegativity approach: applications to silicate and aluminosilicate structures. *Journal of American Chemical Society*, **107**, 6769–6775.

Kanehashi, K. and Saito, K. (2002) Structural analysis of boron compounds using ^{11}B-3QMAS solid state NMR. *Journal of Molecular Structure*, **602**, 105–113.

Kanehashi, K., Saito, K. and Sugisawa, H. (2000) Structural analysis of boron carbide using 2D ^{11}B-MQMAS NMR. *Chemistry Letters*, 588–589.

Khan, M.M.T., Samad, S.A., Siddiqui, M.R.H., Bajaj, H.C. and Ramachandraiah, G.. (1991) Formation of a rhodium(II) monohydrido complex derived from Wilkinson's complex $RhCl(PPh_3)_3$ in the interlamellar spaces of montmorillonite and catalytic hydrogenation of cyclohexene. *Polyhedron*, **10**, 2729–2736.

Kundla, E., Samoson, A. and Lippmaa, E. (1981) High-resolution NMR of quadrupolar nuclei in rotating solids. *Chemical Physics Letters*, **83**, 229–232.

Lippmaa, E., Mägi, M., Samson, A., Engelhardt, G. and Grimmer, A.R. (1980) Structural studies of silicates by solid-state high-resolution ^{29}Si NMR. *Journal of American Chemical Society*, **102**, 4889–4893.

Massiot, D., Touzo, B., Trumeau, D., Coutures, J.P., Virlet, J., Florian, P. and Grandinetti, P.J. (1996) Two-dimensional magic-angle spinning isotropic reconstruction sequences for quadrupolar nuclei. *Solid State Nuclear Magnetic Resonance*, **6**, 73–83.

Mastalir, Á., Király, Z., Szörgy, G. and Bartók, M. (2001) Stereoselective hydrogenation of 1-phenyl-1-pentyne over low-loaded Pd-montmorillonite catalysts. *Applied Catalysis A: General*, **213**, 133–140.

Mooney, R.W., Keenan, A.G. and Wood, L.A. (1952) Adsorption of water vapor by montmorillonite. II. Effect of exchangeable ions and lattice swelling as measured by X-ray diffraction. *Journal of American Chemical Society*, **74**, 1371–1374.

Müller, D., Gessner, W., Behrens, H.J. and Scheler, G. (1981) Determination of the aluminium coordination in aluminium-oxygen compounds by solid-state high-resolution ^{27}Al NMR. *Chemical Physics Letters*, **79**, 59–62.

https://doi.org/10.1346/CCMN.2003.0510505 Published online by Cambridge University Press

Rocha, J. (1999) Single- and triple-quantum ^{27}Al MAS NMR study of the thermal transformation of kaolinite. *Journal of Physical Chemistry B*, **103**, 9801–9804.

Saito, K., Kanehashi, K. and Komaki, I. (2001) Applications of NMR techniques to coal science. *Annual reports on NMR Spectroscopy*, **44**, 23–72.

Staunton, S. and Quiquampoix, H. (1994) Adsorption and conformation of bovine serum albumin on montmorillonite: modification of the balance between hydrophobic and electrostatic interactions by protein methylation and pH variation. *Journal of Colloid and Interface Science*, **166**, 89–94.

Stebbins, J.F., Zhao, P., Lee, S.K. and Oglesby, J.V. (2001) Direct observation of multiple oxygen sites in oxide glasses: recent advances from triple-quantum magic-angle spinning nuclear magnetic resonance. *Journal of Non-Crystalline Solids*, **293**, 67–73.

(*Received 10 September 2002; revised 25 March 2003; Ms. 713; A.E. Randall T. Cygan*)